

DNS OF STOCHASTICALLY FORCED LAMINAR PLANE COUETTE FLOW: PECULIARITIES OF HYDRODYNAMIC FLUCTUATIONS

G. Chagelishvili

Center for Plasma Astrophysics,
Abastumani Astrophysical Observatory,
Kazbegi Ave. 2A, Tbilisi, Georgia
g.chagelishvili@astro-ge.org

Martin Oberlack & George Khujadze

Department of Mechanical Engineering,
Group of Fluid Dynamics, Petersenstr. 13,
Darmstadt, Germany
oberlack@fdy.tu-darmstadt.de & khujadze@fdy.tu-darmstadt.de

ABSTRACT

The background of three dimensional (3D) hydrodynamic/vortical fluctuations in a stochastically forced, laminar, incompressible, plane Couette flow is simulated numerically. The fluctuating field is anisotropic and has well pronounced peculiarities: (i) the hydrodynamic fluctuations exhibits non-exponential, transient growth; (ii) fluctuations with the streamwise characteristic length-scale about two times larger than the channel width are predominant in the fluctuating spectrum instead of streamwise constant ones; (iii) nonzero cross-correlations of velocity (even streamwise-spanwise) components appear; (iv) stochastic forcing destroys the spanwise reflection symmetry (inherent to the linear and full Navier-stokes equations in a case of the Couette flow) and causes an asymmetry of the dynamical processes. The wavelet analysis was used for post-processing of the DNS data. Coherent vortex extraction method was used to split the velocity and vorticity fields in coherent and incoherent parts. The wavelet analysis confirms the existence of the non-constant streamwise coherent structures in the flow.

INTRODUCTION

Stochastically forced Couette flow represents the simplest macroscopic non-equilibrium system in which there are impregnated processes, having microscopic origin (e.g. molecular chaotic motion). The mean flow Reynolds number (Re) provides a single, control and combined parameter to measure the departure of the fluid from its equilibrium state. Investigation of this simple macroscopic non-equilibrium system is of interest from both, general (physical) and peculiar (hydrodynamic/turbulence) standpoints. The hydrodynamic equations describe the macroscopic flow with high accuracy. However, a microscopic foundation of the fluid mechanics has not been well established yet. The investigation of this simplest flow system contributes to make up for this physical deficiency. As for the interest from a hydrodynamic point of view, it has increased during the last decade parallel with the progress that was happening in the comprehension of the basis of the dynamical processes in smooth nonuniform/shear flows, in particular, in the comprehension of the transient extraction of the mean flow energy by perturbations, despite the exponential stability of all normal modes of the system. Specifically, it

was precisely proved in 1990's (Reddy et al. 1993; Reddy and Henningson 1993; Trefethen et al. 1993; Gebhardt and Grossmann 1994; Baggett et al. 1995), that the transient growth of perturbations is due to the non-normality of the linearized dynamical operators of shear flow systems. At the same time, it came the understanding that stochastic forcing is inherent for the environmental and engineering flow systems. These circumstances triggered the recent studies (Farrell and Ioannou 1994; Farrell and Ioannou 1993; Eckhardt and Pandit 2003; Faisst and Eckhardt 2003; Bamieh and Dahleh 2001; Chagelishvili and Khujadze 1997), where it has been proven that different (relatively small) stochastic forcing of a Couette flow even in the linear regime leads to an eddy variance, that greatly exceed the variance levels resulting from the balance between energy accumulated from stochastic forcing and energy dissipated by the normal modes. According to these studies, a consequence of the non-normality of the dynamics of shear flows – transient extraction of the background shear energy by eddy fluctuations – significantly contributes to producing and maintaining this high level of the variance. (On the other hand, without stochastic forcing the perturbation field would vanish.) This significant amplification of variance suggests a fundamentally linear mechanism underlying shear flow turbulence. In Refs. Farrell and Ioannou (1993), Farrell and Ioannou (1994) at the forming of the stochastically forced background, the predominant mechanism is considered the streamwise constant eddies which variance/energy growth was evaluated as $O(Re^3)$, while for streamwise non-constant eddies it was evaluated as $O(Re^{3/2})$ (Chapman 2002).

The aims of this paper are calculation of the fluctuating background of the stochastically forced plane Couette flow using DNS. One of the main object of the study is to define characteristic configurations and length scales of the fluctuation background. To verify or refute the predominance of streamwise constant vortices, to calculate correlations and cross-correlations between fluctuating velocity components were also addressed in this study. As intrinsic to the stochastic flow forcing we consider a random stress tensor which satisfies the fluctuation-dissipation theory relation (Landau and Lifshitz 1980). The results shown in this paper were partly presented in Khujadze et al. (2006).

Wavelet analysis was used for the postprocessing of the numerical data. The wavelet transform has been found to be particularly useful for analysing signals which can best

be described as aperiodic, noisy, intermittent, transient and so on. Its ability to examine the signal simultaneously in both time and frequency in a distinctly different way from the traditional short time Fourier transform has initiated a number of wavelet-based methods for signal manipulation and interrogation. One of a such method, called coherent vortex extraction (CVE) developed by Farge et al. (2001) was used in our study (more details about the method see in the last section).

STOCHASTIC LINEAR NAVIER-STOKES EQUATIONS

Consider an incompressible, plane Couette flow ($\mathbf{U}_0 = (Ax_2, 0, 0)$) in 3D with shear parameter A , channel half-width L and Reynolds number Re , that is based on the mean centreline velocity and the half-width of the channel ($Re \equiv AL^2/\nu$). In the laminar case ($Re < 350$) the Couette flow is slightly non-equilibrium and the fluctuations can be neglected beyond the *linear* order. Consequently, the linearized equations for small stochastic forced fluctuations can be written in Cartesian coordinates as

$$\frac{\partial u_i(\mathbf{r}, t)}{\partial x_i} = 0 \quad (1)$$

$$\left(\frac{\partial}{\partial t} + Ax_2 \frac{\partial}{\partial x_1} \right) u_i(\mathbf{r}, t) + Au_2(\mathbf{r}, t)\delta_{i1} = -\frac{1}{\rho_0} \frac{\partial p(\mathbf{r}, t)}{\partial x_i} + \nu \Delta u_i(\mathbf{r}, t) + \frac{\partial s_{ij}(\mathbf{r}, t)}{\partial x_j} \quad (2)$$

where ρ_0 is the uniform fluid density, $u_i(\mathbf{r}, t)$ and $p(\mathbf{r}, t)$ are the components of the velocity fluctuations ($i = 1, 2, 3$) and the pressure fluctuations respectively, Δ is the Laplacian and $s_{ij}(\mathbf{r}, t)$ corresponds to the spontaneous strain tensor. The last term containing $s_{ij}(\mathbf{r}, t)$ defines the stochastic forcing of the system. Statistical properties of the spontaneous strain tensor are modelled in accordance with the Fluctuation-Dissipation theory Landau and Lifshitz (1980):

$$\langle s_{ij}(\mathbf{r}, t) s_{kl}(\mathbf{r}', t') \rangle = \frac{2T\nu}{\rho_0} \left[\delta_{ik}\delta_{jl} + \delta_{il}\delta_{kj} - \frac{2}{3}\delta_{ij}\delta_{kl} \right] \delta(\mathbf{r} - \mathbf{r}')\delta(t - t') \quad (3)$$

The no-slip boundary conditions are:

$$u_i(x_1, \pm L/2, x_3, t) = 0 \quad (4)$$

Our numerical code needs the definition of the stochastic forcing in mixed spectral-physical space, i.e. in spectral coordinates in the streamwise (x_1) and spanwise (x_3) directions, and in physical coordinates in the wall-normal (x_2) direction. Using Fourier transform:

$$s_{ij}(\mathbf{r}, t) = \int d\mathbf{k} S_{ij}(\mathbf{k}, t) \exp(i\mathbf{k}\mathbf{r}) \quad (5)$$

one gets:

$$\langle S_{ij}(\mathbf{k}, t) S_{kl}(\mathbf{k}', t') \rangle = \frac{2T\nu}{\rho_0} \left[\delta_{ik}\delta_{jl} + \delta_{il}\delta_{kj} - \frac{2}{3}\delta_{ij}\delta_{kl} \right] \delta(\mathbf{k} - \mathbf{k}')\delta(t - t') \quad (6)$$

The realization of $S_{ij}(\mathbf{k}, t)$ that satisfies the statistic characteristics of Eq. 6 is given in Appendix (see equation 8).

DNS OF THE FLOW

The code for the DNS was developed at KTH, Stockholm (for details see Skote (2001)) using a spectral method

with Fourier decomposition in the horizontal directions and Chebyshev discretization in the wall-normal direction. Time integration is performed using a third-order Runge-Kutta scheme for the advective and forcing terms and Crank-Nicolson for the viscous terms. The transformation between physical and spectral space is done by Fast Fourier Transformation. Simulations were performed on the IBM supercomputer (Regatta-H) at Technische Universität Darmstadt, Germany. To perform numerical simulation of the channel flow with hydrodynamic fluctuation background, the code was modified implementing stochastic forcing (equation 8) satisfying the condition of fluctuation-dissipation theory (equation 6).

Two simulations were performed for the flow. First of all, the linear Navier-Stokes equations with the stochastic forcing were numerically simulated on the box ($L_{x_1} = 6\pi$) \times ($L_{x_2} = 2$) \times ($L_{x_3} = 2\pi$) using the following grid: $256 \times 217 \times 128$. The simulation was performed using the parameters: $[L] = 1$, $[\nu] = 1/300$ and $[A] = 0.3; 1; 3$, i.e. for $Re = 90; 300; 900$, which reproduce literature values for the linearized problem. The initial flow-field perturbations are set to zero. Consequently, in the system flow-field perturbations are solely due to the stochastic forcing. The performed linear simulations show that variance reaches a finite statistically stationary level at $[t] > 150$. This level largely exceeds the variance levels resulting from the balance between energy accumulated from stochastic forcing and energy dissipated by the normal modes. This fact is in agreement with the recent studies of a stochastically forced shear flows (Farrell and Ioannou 1994; Farrell and Ioannou 1993; Eckhardt and Pandit 2003; Bamieh and Dahleh 2001; Chagelishvili and Khujadze 1997). The reason of this is a transient extraction of the background shear energy by the eddy fluctuations that is a consequence of the non-normality of channel flows linear dynamics.

The next step was to verify the results of the DNS of the linear equations performing DNS of the full non-linear Navier-Stokes equations with the same stochastic force at very small amplitudes (namely, at $\epsilon = 10^{-3}$), for which the nonlinear forces are not at work. This non-linear simulation confirmed the linear dynamical picture. Here we present some qualitative and quantitative results (demonstrating key features of the fluctuating background) by means of Figs. 1-4.

Velocity fields of statistically stationary fluctuating background in different planes are illustrated in Fig. 1: Configurations of u_1 , u_2 and u_3 , on a $x_1 - x_2$ plane at $x_3 = 0$ are presented respectively in Figs. 1a-c. (The configurations are the same for different values of x_3 .) Additionally, configuration of u_1 on a $x_1 - x_3$ plane at $x_2 = 0$ is presented in Fig. 1d. Black (white) areas relate to the positive (negative) values of u_i . As one can see, the fluctuating background is chaotic, but definite regularities are obviously traced. One observes that these regularities – different configurations and scales – are different for the different components of the velocity fluctuations. This points out the differences between the dynamics of the different components. In fact, provided that the components grow by classical/unitary exponential law, the final configurations of the components should be similar to each other. However, when perturbations extract the shear energy due to the flow non-normality, the different components of velocity perturbation extract the energy not by unitary/exponential law, but by algebraic laws each of which is different to each other. This circumstance leads to different characteristic configurations and scales of the velocity components at the final balance that is seen in Figs.

1a-d.

Figs. 1a,d and 2 also point out another particularity: the dominating fluctuations in the background are not streamwise constant fluctuations (as it is supposed in (Farrell and Ioannou 1994; Farrell and Ioannou 1993; Eckhardt and Pandit 2003; Bamieh and Dahleh 2001)), but eddies prolonged in the streamwise direction ($\langle u_1^2 \rangle \gg \langle u_2^2 \rangle, \langle u_3^2 \rangle$). The characteristic streamwise length scale of u_1 is about two times larger than the channel width. This numerical fact is the obvious. The channel width is the only macroscopic length scale in the system and it should define the characteristic streamwise length scale of eddies as it exists. Physically, this fact is due to the action of the channel boundaries and is conformed with the non-normality of the flow. To discuss this problem we borrow the knowledge about non-normal linear processes in unbounded shear flow from Ref. Chagelishvili and Khujadze (1997) and about the action of the channel boundaries from Refs. S.Marcus and W.H.Press (1977), Criminale and Drazin (1990) and W.O.Criminale et al. (1997).

According to Chagelishvili and Khujadze (1997), in stochastically forced unbounded constant shear flows, the linear regime, statistically stationary level variance at different streamwise length scale (l_x) is achieved independently of each other. The characteristic time scale is defined by $\tau(l_x) \approx l_x/\sqrt{A\nu}$. The levels achieved are significantly increased with $\tau(l_x)$, i.e. with l_x for a fixed A and ν . The achievement of the steady state solution should be “destroyed” at large l_x by the action of boundaries. Actually, according to Refs. S.Marcus and W.H.Press (1977), Criminale and Drazin (1990) and W.O.Criminale et al. (1997), the rigid boundaries affect the dynamics of perturbations at different l_x independently. Analyzing the linear problem with Kelvin modes (Kelvin 1887, Craik and Criminale (1986)), one can say, that at the dynamics of initial/original perturbations, boundaries induce “secondary” perturbations with the same l_x to cancel the “original” perturbations on the boundaries (to satisfy no-slip boundary conditions, see equation 4). The process of the induction of the “secondary” perturbations has the following features:

- the characteristic time scale of the generation of the secondary perturbations is similar for all l_x ($\tau_b(l_x) \approx \text{constant}$), while the intensity is higher, for larger l_x ;
- the phases of the secondary perturbations and the original ones are distinct. The interference between original and secondary perturbations would be destructive.

From the aforesaid it might be concluded that the secondary perturbations weaken the original perturbations due to the interference. The weakening is negligible for small l_x when $\tau(l_x) \ll \tau_b(l_x)$, however significantly affects on the level of perturbations for large l_x when $\tau(l_x) \gtrsim \tau_b(l_x)$. One can deduce that the boundaries “cuts off” large length scale fluctuations at some l_x^{max} for which $\tau(l_x^{max}) \approx \tau_b(l_x^{max})$. Thus, no-slip boundary conditions prevent the dominance of the streamwise constant fluctuations as was conjectured in Refs. Farrell and Ioannou (1993), Farrell and Ioannou (1994), Eckhardt and Pandit (2003) and Bamieh and Dahleh (2001). According to the performed DNS, l_x^{max} is about two times larger than the channel width (see Figs. 1a,d).

Note that some structural regularities traced on Figs. 1a-d should not be considered as three-dimensional stationary/coherent structures similar to the ones reported in Refs. Faisst and Eckhardt (2003), Wedin and Kerswell (2004) and Fitzgerald (2004). However, they may be considered as roots/seeds of these nonlinear coherent structures.

The performed numerical simulations revealed an anisotropy of the fluctuating velocity field that increases

with the shear rate. The anisotropy (measured by $\langle u_2^2 \rangle / \langle u_1^2 \rangle$ and $\langle u_3^2 \rangle / \langle u_1^2 \rangle$) vs x_2 at $A = 1; 3$ is presented in Fig. 2. One can see, that the $\langle u_2^2 \rangle / \langle u_1^2 \rangle$ anisotropy is more profound than $\langle u_3^2 \rangle / \langle u_1^2 \rangle$ anisotropy and increases with the shear rate.

Normalized cross-correlations of the fluctuating velocity components at $A = 1$ are presented in Fig. 3. One can see that the value of streamwise–spanwise cross-correlation exceeds the value of streamwise–cross stream cross-correlation ($|\langle u_1 u_3 \rangle| > |\langle u_1 u_2 \rangle|$). The existence of non-zero streamwise–wall-normal cross-correlation is apparently connected to the breaking of the spanwise reflection symmetry (inherent to the linear and full Navier-stokes equations in the case of a Couette flow) by the stochastic forcing. The later causes an asymmetry of equation 2 and, consequently, an asymmetry of the dynamical processes.

Another consequence of the reflection symmetry breaking is also well profound in Fig. 4, where the fluctuation energy on a $x_1 - x_3$ plane at $x_2 = 0$ is presented. Black (white) areas relate to the values of the energy greater (smaller) than the value $2.7 \cdot 10^{-7}$. As one can see, the energy (and, consequently, the fluctuations) has no spanwise reflection symmetry.

WAVELETS: COHERENT VORTEX EXTRACTION

As it was presented in the previous sections, the flow exhibits organized structures developing in the fluctuation background. A separation of the flow field into coherent and incoherent part helps in the understanding of the shear flow phenomena in a stochastically forced flow. The so-called CVE developed by authors Farge et al. (2001) was used for this aim. The principle of CVE is to split a flow into a coherent and incoherent parts. About the details of CVE one see the paper by Schneider et al. (2006). Here we just give brief introduction into the method taken from this paper. The idea is to apply denoising algorithm to the vorticity field ω given at resolution N at a given time instant t . The decomposition gives $\omega = \omega_C + \omega_I$, that means coherent ω_C and incoherent ω_I parts respectively. Using 3D wavelet decomposition by applying Fast Wavelet Transform (FWT), we transform each component of vorticity vector in the wavelet space $\tilde{\omega}$, then compute the threshold $\varepsilon_T = \sqrt{\frac{4Z}{3} \ln N}$ (the threshold only depends on the total enstrophy $Z = \frac{1}{2} \int |\omega|^2 dx$ and on the number of grid points N) and split vorticity components in wavelet space into

$$\tilde{\omega}_C = \begin{cases} \tilde{\omega} & \text{for } |\tilde{\omega}| > \varepsilon_T \\ 0 & \text{otherwise} \end{cases} \quad \tilde{\omega}_I = \begin{cases} \tilde{\omega} & \text{for } |\tilde{\omega}| \leq \varepsilon_T \\ 0 & \text{otherwise} \end{cases} \quad (7)$$

and the next step is 3D wavelet reconstruction by applying inverse FWT to compute ω_C and ω_I . Due to the orthogonality: $\langle \omega_C, \omega_I \rangle = 0$ that ensures that $Z = Z_C + Z_I$.

Applying the curl operator ($\mathbf{v} = (\nabla \times)^{-1} \omega$) we obtain the corresponding velocity fields: $\mathbf{v} = \mathbf{v}_C + \mathbf{v}_I$.

Figs. 5, 6, 7, 8 and 9 show the results of the CVE usage on the velocity, energy and vorticity fields. The top and bottom plots in these figures show the coherent and incoherent parts (white noise) of the fields correspondingly. As we see, the main part of the energy of a fluctuation background is located in the coherent part. Incoherent part is white noise. The coherent structures of the velocity field are different for the different components of velocity vector. This fact validates the results obtained by the DNS of the flow: non-exponential, transient behaviour of the perturbations. Comparing Figs. 5 and 8 we see that the main part of energy is containing in the streamwise velocity which

is dominant on the spanwise and wall-normal components. Fig. 9 shows the coherent and incoherent parts of the vorticity modulus $|\omega|$. The vorticity field is more smooth and it contains more localized structures than the velocity field. The non-constant streamwise oriented vortical structures are displayed in this figure. No organized structures are left in the incoherent part of the field.

SUMMARY

Let's summarize the DNS of Navier-Stokes equations at small amplitude (linear) stochastic forcing. The performed simulations revealed the evident peculiarities of statistically stationary fluctuating field of a laminar plane Couette flow. Especially, they show:

- The non-normal (non-exponential) growth of the hydrodynamic perturbations – the finite statistically stationary level is defined by the non-normality of the non-equilibrium flow system;
- An anisotropy of the fluctuating velocity field ($\langle u_1^2 \rangle \gg \langle u_2^2 \rangle, \langle u_3^2 \rangle$), that increases with the shear rate;
- Dominance of the streamwise *non-constant* fluctuations. (I.e., non-dominance of the streamwise *constant* fluctua-

tions.) The characteristic scale of the main component of the velocity fluctuations (u_1) is about two times larger than the channel width. This dominance should be important for correlations (especially, for asymmetric time correlations Eckhardt and Pandit (2003));

- Appearance of nonzero cross-correlations of velocity (even streamwise-spanwise) components;
- Spanwise reflection symmetry breaking due to the dynamical processes.

One may also conclude the existence of some structural regularities in the fluctuating background that can be considered as a seed of some recently observed nonlinear stationary/coherent structures Fitzgerald (2004).

ACKNOWLEDGEMENT

G.Kh. would like to thank Profs. M. Farge and K. Schneider (France) for introducing him in the fascinating world of Wavelets and allowing him to use the CVE code developed by them. We would like to express the gratitude to Profs. Henningson and Johansson from KTH, Stockholm for given to us an opportunity the use their code for DNS developed in their groups.

APPENDIX

$$S_{ij}(\mathbf{k}, t) \equiv \epsilon \left\{ \begin{array}{ccc} \sqrt{\frac{4}{3}} \cos[2\pi\phi_1(\mathbf{k}, t)] & \cos[2\pi\phi_2(\mathbf{k}, t)] & \cos[2\pi\phi_3(\mathbf{k}, t)] \\ \cos[2\pi\phi_2(\mathbf{k}, t)] & \sqrt{\frac{4}{3}} \cos[2\pi\phi_1(\mathbf{k}, t) + \frac{2}{3}\pi] & \cos[2\pi\phi_4(\mathbf{k}, t)] \\ \cos[2\pi\phi_3(\mathbf{k}, t)] & \cos[2\pi\phi_4(\mathbf{k}, t)] & \sqrt{\frac{4}{3}} \cos[2\pi\phi_1(\mathbf{k}, t) + \frac{4}{3}\pi] \end{array} \right\} \quad (8)$$

where $\epsilon \equiv \sqrt{8T\nu/\rho_0}$ is a measure of the stochastic forcing, $\phi_1(\mathbf{k}, t)$, $\phi_2(\mathbf{k}, t)$, $\phi_3(\mathbf{k}, t)$, $\phi_4(\mathbf{k}, t)$ are random numbers in the range $[0, 1]$ different for different \mathbf{k} and t .

REFERENCES

- Baggett, J., T. Driscoll, and L. Trefethen (1995). sddfd-fgfwe. *Phys. Fluids* 7, 833.
- Bamieh, B. and M. Dahleh (2001). Energy amplification in channel flows with stochastic excitation. *Phys. Fluids* 13, 3258.
- Chagelishvili, G. and G. Khujadze (1997). Fluctuation background due to incompressible disturbances in laminar shear flows. *JETP* 85, 907.
- Chapman, S. J. (2002). Subcritical transition in channel flows. *J. Fluid Mech.* 451, 35–97.
- Craik, A. and W. Criminale (1986). Evolution of wavelike disturbances in shear flow: a class of exact solutions of the navier-stokes equations. *Proc. R. Soc. (London) A* 406, 13.
- Criminale, W. and P. Drazin (1990). sdsad. *Studies in Applied Mathematics* 83, 123.
- Eckhardt, B. and R. Pandit (2003). Noise correlations in shear flows. *European Phys. J. B* 33, 373.
- Faisst, H. and B. Eckhardt (2003). Traveling waves in pipe flow. *Phys. Rev. Lett.* 91, 224502.
- Farge, M., G. Pellegrino, and K. Schneider (2001). Coherent vortex extraction in 3d turbulent flows using orthogonal wavelets. *Phys. Rev. Lett.* 87(5), 054501.
- Farrell, B. and P. Ioannou (1993). Stochastic forcing of linearized navier-stokes equations. *Phys. Fluids A* 5, 2600.
- Farrell, B. and P. Ioannou (1994). dwerdtgdr. *Phys. Rev. Lett.* 72, 1188.
- Fitzgerald, R. (2004). New experiments set the scale for the onset of turbulence in pipe flow. *Physics Today*.
- Gebhardt, T. and S. Grossmann (1994). Chaos transition despite linear stability. *Phys. Rev. E* 50, 3705.
- Kelvin, L. (1887). *Philos. Mag.* 23, 459.
- Khujadze, G., M. Oberlack, and G. Chagelishvili (2006). Direct numerical simulation of stochastically forced laminar plane couette flow: Peculiarities of hydrodynamic fluctuations. *Phys. Rev. Letters* 97, 034501.
- Landau, L. and E. Lifshitz (1980). *Statistical Physics*. Pergamon Press.
- Reddy, S. and D. Henningson (1993). Energy growth in viscous channel flow. *J. Fluid Mech.* 252, 209.
- Reddy, S. C., P. J. Schmid, and D. S. Henningson (1993). Pseudospectra of orr-sommerfeld operator. *SIAM J. Appl. Math.* 53, 15.
- Schneider, K., M. Farge, A. Azzalini, and J. Ziuher (2006). Coherent vortex extraction and simulation of 2d isotropic turbulence. *Journal of Turbulence* 7(44).

Skote, M. (2001). *Studies of turbulent boundary layer flow through direct numerical simulation*. Ph. D. thesis, Royal Institute of Technology, Stockholm, Sweden.

S.Marcus and W.H.Press (1977). On green's functions for small disturbances of plane couette flow. *J. Fluid Mech.* 79, 525.

Trefethen, L., A. Trefethen, S. Reddy, and T. Driscoll (1993). Hydrodynamic stability without eigenvalues. *Science* 261, 578–584.

Wedin, H. and R. R. Kerswell (2004). Exact coherent structures in pipe flow: travelling wave solutions. *J. Fluid Mech.* 508, 333.

W.O.Criminale, T.L.Jackson, D.G.Lasseigne, and R.D.Joslin (1997). Perturbation dynamics in viscous channel flows. *J. Fluid Mech* 339, 55.

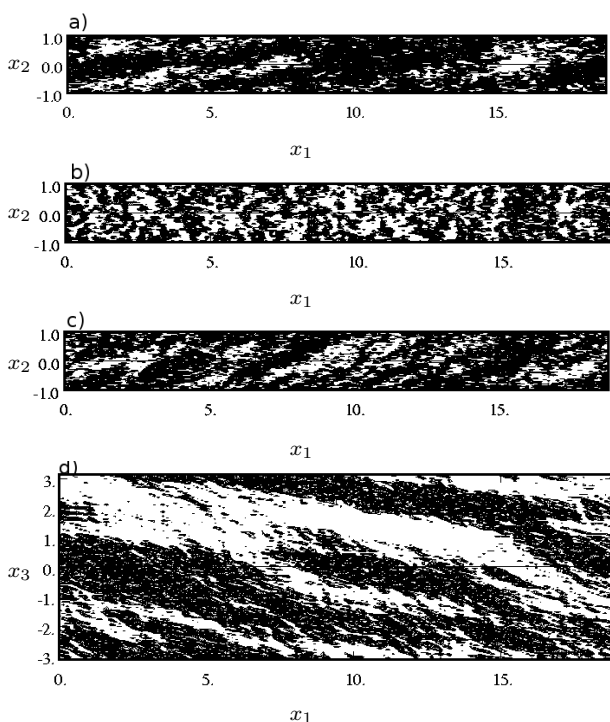


Figure 1: Velocity fields of the established fluctuating background in different planes. (a,b,c) u_1 , u_2 and u_3 respectively in the x_1-x_2 plane at $x_3=0$. (d) u_1 in the x_1-x_3 plane at $x_2=0$. Black (white) areas relate to the positive (negative) values of u_i .

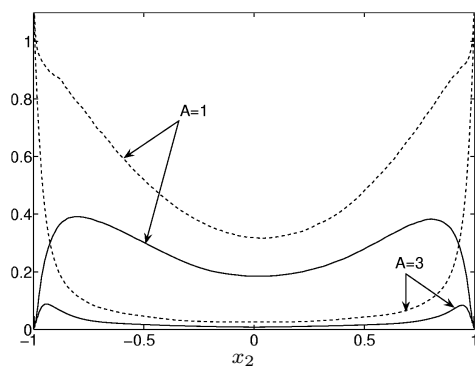


Figure 2: — $\langle u_2^2 \rangle / \langle u_1^2 \rangle$, --- $\langle u_3^2 \rangle / \langle u_1^2 \rangle$ vs x_2 at $A=1;3$.

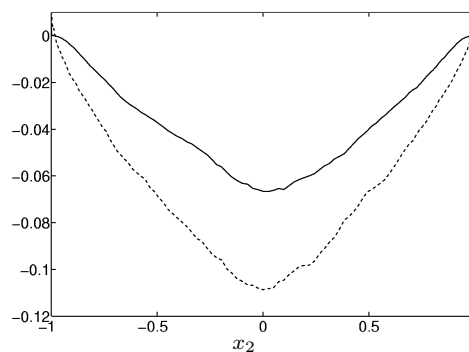


Figure 3: — $\langle u_1 u_2 \rangle / \alpha$, --- $\langle u_1 u_3 \rangle / \alpha$ vs x_2 at $A=1$. $\alpha \equiv \langle u_1^2 \rangle |_{x_2=0}$.

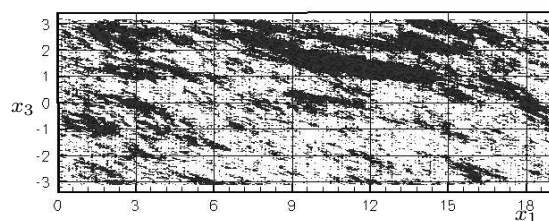


Figure 4: The fluctuation energy on a x_1-x_3 plane at $x_2=0$. Black (white) areas relate to the values of the energy greater (smaller) than the value $2.7 \cdot 10^{-7}$.

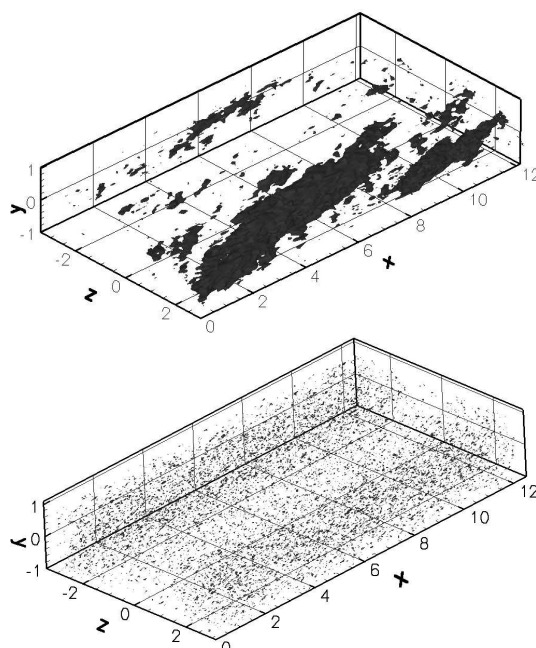


Figure 5: Streamwise velocity: Coherent u_{1C} (top plot) and incoherent u_{1I} (bottom plot) parts.

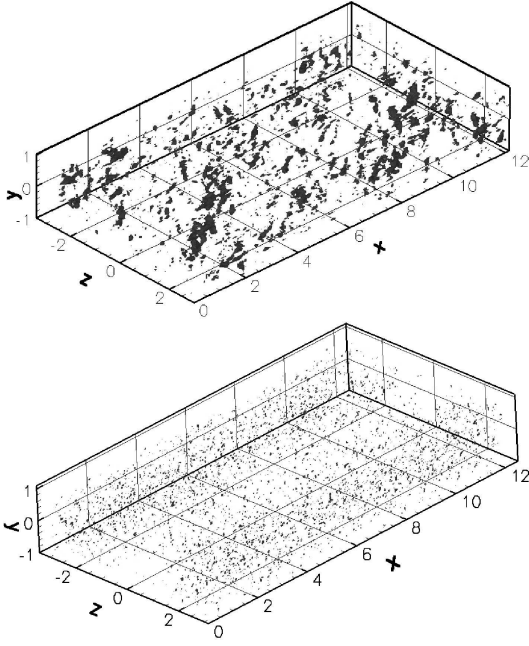


Figure 6: Wall-normal velocity: Coherent u_{2C} (top plot) and incoherent u_{2I} (bottom plot) parts.

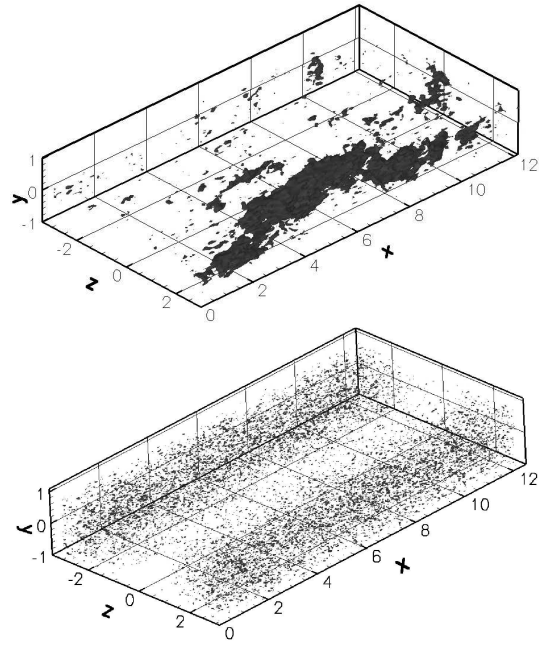


Figure 8: Energy field $E \approx E_C + E_I$: Coherent and incoherent parts.

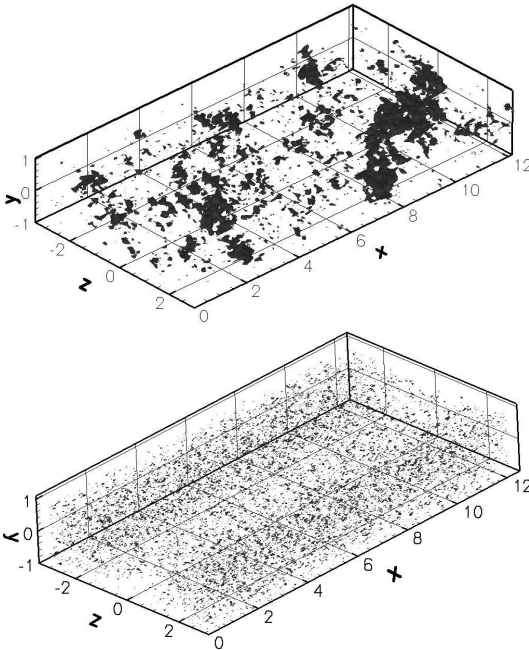


Figure 7: Spanwise velocity: Coherent u_{3C} (top plot) and incoherent u_{3I} (bottom plot) parts.

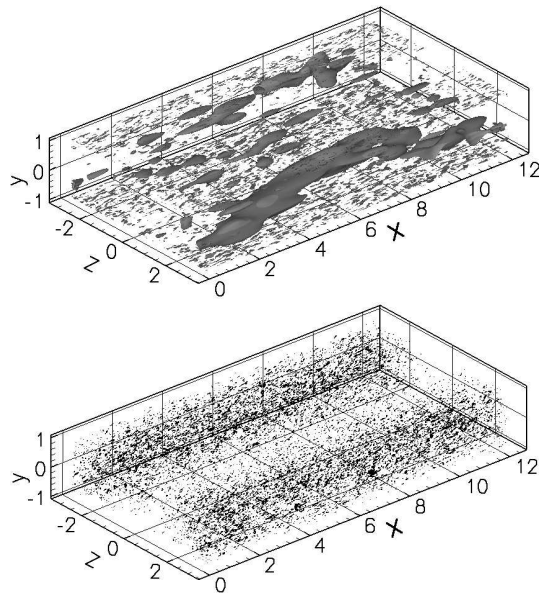


Figure 9: Modulus of vorticity ($|\omega|$): Coherent $|\omega|_C$ (top plot) and incoherent $|\omega|_I$ (bottom plot) parts.